

Exploring sensor fusion in odometry to improve robot localisation

Tushar Bhatnagar(97607) Jasmeet Khalsa(97313) Samia Mohinta(97293) Tanya Sharma(15606)

Abstract—This project involves experimentation with a robotic system which has been assigned a task of exploring an uncharted but demarcated undersea environment that contains a sunken ship loaded with treasure. In order to assist this autonomous navigation and simultaneously build a map of the environment, this project aimed at investigating odometry and improving the localisation of the robot. Particularly, two major types of odometric errors, systematic and non-systematic/random, have been investigated to minimize the overall error in odometry. To reduce the impacts of these errors on the position estimate of the robot, the effects of calibration and sensor fusion have been analysed. Experimentally, the project has examined wheel odometry with sensor fusion to estimate the robot's accuracy in relative positioning. Two tests have been performed to calculate the odometric error in terms of translation error and orientation error: 'UMBmark test' and 'Random-walk, Go Home test'. A complementary filter has been adapted to calculate the heading estimate in sensor fusion. Analysis of the experimental findings demonstrate significant improvement in odometric accuracy of the calibrated robot on integration of sensor fusion with wheel encoders.

I. INTRODUCTION

Accurate localisation of a robot, which is a robot's ability to keep track of where it is in an environment, seems to be a fundamental challenge in mobile robot applications for navigation and exploration [1]. The most widely used technique to estimate a mobile robot's position is wheel odometry [2]. Wheel revolutions can be translated to linear displacement of the robot from a specific point, while encoders can be used to measure wheel rotation. However, owing to the fact that odometry is based on the integration of incremental motion information over time, it is prone to accumulating error over time.

The experimental scenario consists of exploring and mapping different features in an unknown undersea area, which is believed to contain a sunken ship with treasure. The aim of this project is to examine and improve odometry subsystem to facilitate optimum navigation, thereby enabling the robot to encode a better map.

The prime motivation behind investigating this subsystem was not only dependent on the current experimental scenario but also from the observations made during the 'Go Home' section of the first coursework. Every time the experiment was performed for coursework 1, the robot presumed the 'home' location to be different, based on its relative starting point. This prompted us to study this relative position estimation that is affected by odometry errors of the mobile robot system.

Sources of odometry error are categorised into systematic errors and non-systematic/random errors [3][4]. Systematic errors are system (robot) specific and usually remain con-

stant during navigation. These are mainly caused by the wheel's kinematic modelling errors. The most significant error sources are unequal wheel diameters and incorrect wheelbases. On the other hand, non-systematic/random errors are mainly influenced by the actual environment. In the real world, systems are affected by fluctuations in several environmental parameters such as surface texture, temperature, pressure, humidity, vibrations and magnetic field. As a result, non-systematic/random errors are generally unpredictable, preventing anticipation of remediation.

There are various techniques for measuring and evaluating these errors. In this project, calibration, which is a proposed way of counteracting systematic error [5], is implemented to overcome predictable errors in the sensors. Secondly, to diminish the effects of non-systematic/random errors in odometry, sensor fusion [6] is used. Odometry based on wheel encoders, fusion of gyroscope and magnetometer, fusion of magnetometer and kinematics and fusion of gyroscope and kinematics for orientation estimates [7] has been investigated. Gyroscope (inside the IMU) measures the angular velocity of the robot. Orientation estimates can be calculated by integrating this angular velocity with respect to time. However, since gyroscopes are prone to drift [8], this integration can accumulate error. Small errors in angular velocity can compound to a significant error when integrated over time, thereby leading to incorrect position estimates[9].

Using a magnetometer is another alternative for measuring the heading of the robot. Since the absolute measure of this sensor is used (i.e. no integration is required) for heading estimation, the accuracy in measurement is much higher than gyroscope after a certain period of time. A magnetometer is initially slow in orienting itself with the true magnetic north but can give an improved and consistent heading estimate over a prolonged duration of time. The values from the magnetometer also fluctuate when the robot is in motion and can only give an absolute and precise estimate when it is stationary. The magnetometer used in our experiments has an accuracy of $\pm 10^\circ$.

Two different tests were designed and organised to assess the performance of odometry. A 'Random-walk, Go Home' test and a 'University of Michigan Benchmark (UMBMark)' test [10][11] is conducted to test the aforementioned different combinations of sensors. Our experiments made use of wheel encoders for travelling and rotating from one position to another both in 'Random-walk, Go Home' and 'UMBmark' tests with heading determined from the sensor combinations.

The following section presents the research methodology adapted for the project. Section III explains the system architecture of the robot. The results from the experiments

have been analysed and discussed in Section IV, followed by the effect of sensor fusion on the map encoded by the robot in Section V. Conclusion in the view of all experimental results are included in Section VI, which paved the way for considering future enhancements in Section VII to have a more comprehensive and accurate understanding of the subsystem's performance in different scenarios.

II. RESEARCH METHODOLOGY

Throughout the course of this project, several different experiments are conducted to study the overall odometric performance, with attempts to understand the different sources that affect this performance. The experiments performed can be broadly classified into two categories - wheel odometry (using wheel encoders for traversal as well as heading angle) and sensor fusion based odometry. Sensor fusion was used for heading angle estimation in both experiments. The movement of the robot and translation to certain positions was always governed using kinematics. Experiment models are described in section A. The experimental set-up and the rationale behind experimental design is described in section B.

A. Experiment Models

1) *Kinematic Model for Wheel Odometry*: Wheel odometry is the most popular method to calculate relative position estimates of a mobile robot [12]. Wheel revolutions are translated into linear displacement and wheel encoders are used to calculate the heading angle estimate. Experiments using kinematics with tuned PID have been performed during coursework 1. The observations during those experiments, with respect to the accumulation of errors, motivates an in-depth study of the kinematics based spatial navigation of the robot.

2) *Magnetometer Model*: Magnetometers [13] are used for finding the orientation of a device with respect to absolute north (direction of the magnetic field of the earth). It measures the heading angle by estimating the local magnetic field. The local magnetic field also includes the magnetic field created due to the presence of magnetic objects. This causes a disturbance in the readings, which to some extent can be mitigated with good calibration. However, the absolute values of the sensor (with a slight variation of $\pm 10^\circ$) from literature has been deemed more reliable than the heading angles calculated from wheel encoders [14].

3) *Gyroscope Model*: Gyroscope [15] measures the angular velocity at time T. To estimate the robot's orientation from the gyroscope, the measurements need to be integrated with respect to time. This can lead to erroneous values, since the measurements are often corrupted with noise due to drift of the robot's wheel and noise in the sensors. This element of noise could be removed through proper calibration, wherein the robot is kept stationary in the desired axis during the calibration process. Calibration, in general, is performed by taking multiple readings, calculating offsets (maximum and minimum values) utilising the sensitivity of respective sensors.

Since no model in itself would give an optimum result, various combinations of fusing wheel encoder, magnetometer and gyroscope are used to find the best odometric performance in the two types of tests conducted. However, for tests with the magnetometer fused with either encoders or gyroscope, the effects of magnetic interference need to be considered. A list of prior considerations are mentioned below:

- The experimental data is collected at two different places, namely Merchant Venturers Building(MVB) and Hodgkin House, to explain the effects of magnetic interference on the heading estimates from the magnetometer.
- Calibration is always performed away from the ground so that the magnetometer can align itself with the true magnetic north.[16]
- All experimentation is conducted on smooth surfaces to avoid surface drift and wheel slippage.

Complementary filter

There are various types of sensor fusion algorithms. These can be explicit or probabilistic (e.g. Kalman filter). The most commonly used explicit sensor fusion algorithm is the complementary filter [17]. As discussed in the previous section, improved accuracy in the estimate of the robot's orientation can be achieved by fusing encoder, gyroscope and/or magnetometer measurements [4]. The complementary filter will use the fact that measurements from the combination of these sensors would provide information about the orientation of the robot.

Initial evaluation of orientation from the gyroscope and magnetometer provides varying measurements. While the magnetometer is noisy but nearly accurate over time, the gyroscope is accurate for a short period of time but accumulates error in longer time periods due to drift. At high frequencies, the gyroscope has desirable measurements, which deteriorate at lower frequencies. Therefore, a high-pass filter (Equation 1) is required to calculate orientation. Similarly, magnetometer readings are less noisy at low frequencies and therefore, a low-pass filter (Equation 2) is required to estimate orientation.

$$output_t = (\alpha * output_{t-1}) + (1 - \alpha) * reading_t \quad (1)$$

$$output_t = \alpha * (reading_t - reading_{t-1}) + (1 - \alpha) * output_{t-1} \quad (2)$$

A complementary filter would provide a combination of the high-pass and low-pass filters to estimate the fused heading angle θ . The equation for the complementary filter can be written as:

$$\theta_t = (1 - \alpha) * \theta_{mag} + \alpha * (\theta_{t-1} + \theta_{gyro} * elapsed_time) \quad (3)$$

B. Experiment Set-up

Sensor fusion and wheel odometry is evaluated after experimental data collection. The experimental set-up for the 'Random-walk, Go Home' test and the 'UMBmark' test is described below.

1) *Random-walk, Go Home*: The first experiment conducted is ‘Random-walk, Go Home’, which entails that the robot randomly walks for a stipulated period of time and then orients itself to return to its starting point on the map. There are 4 trials for each stipulated duration of random walk, which are 10 seconds, 20 seconds and 30 seconds respectively. The return home position coordinates are noted manually on the map with respect to the origin. This experiment enables us to visualize the displacement error build-up over time, measured by taking the distance difference from the start point. However, it is also understood that through this experiment, we are neither able to isolate the translation and orientation error contributions, nor identify the effects of systematic and non-systematic/random error on the total degraded odometric performance.

2) *UMBMark Test*: A University of Michigan Benchmark test [10], is conducted as an improvement to the previous experiment. For the UMBmark test, the robot was programmed to traverse the four legs of a square path in a unidirectional clockwise pattern. The closed path returned the robot to the starting point. Three rounds of the UMBmark test are performed and position coordinates of the robot on reaching four corners of the square are marked manually on the map. Displacement error at each corner of the square is calculated by subtracting the reached coordinates from the true coordinates of that point. Given the design of this experiment, it is assumed that the displacement at each point would be more prominent with respect to kinematic error accumulation over time, which can be visualized in terms of undershooting or overshooting a point and incorrect rotation angles.

III. SYSTEM ARCHITECTURE DIAGRAM

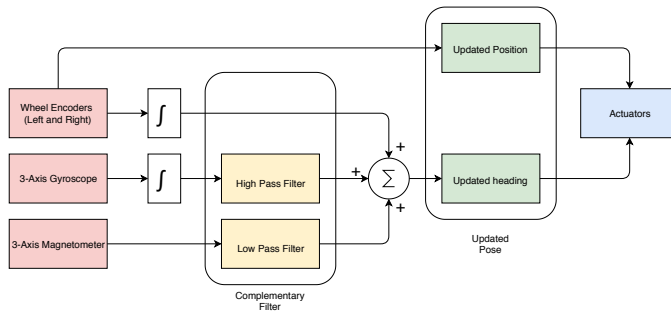


Fig. 1. Hierarchical System Architecture of the investigated subsystem

Figure 1 shows the system architecture, which exemplifies the flow of sensor data to the odometry subsystem and in turn to the actuators.

IV. RESULTS AND DISCUSSION

The metric used all through this section is ‘Position Accuracy’ (displacement error) that is the deviation between the commanded position and the measured position [18][19][20].

A. Baseline Experiment: Random-walk, Go Home

The results from ‘Random-walk, Go Home’ experiment using heading from kinematics are shown in Figure 2. This experiment is performed to demonstrate that the wheel encoders accumulate error as the distance moved increases over different time periods of random walking. From the scatter plot (Figure 2), it can be clearly observed that as the robot travels farther from the origin, its perception of the starting point (home) deteriorates. In particular, it can be visualized that the perceived home positions, where the robot returned after 10 seconds of random walk, have less displacement error, than the perceived home position after 30 seconds of the random walk. The general trend in Figure 3, shows that the displacement error tends to increase with longer time periods of random walking. This noticeable positional drift can be attributed to the unbounded growth of translation and orientation errors due to wheel slippage, floor roughness or discretised sampling of wheel increments.

Nevertheless, the observed pattern of error aggregation can be predicted based on prior experiments with kinematics during the first coursework. This experiment was repeated using sensor fusion of magnetometer and gyroscope to note any improvement in odometric performance, the results from which have been analysed in the following sub-section.

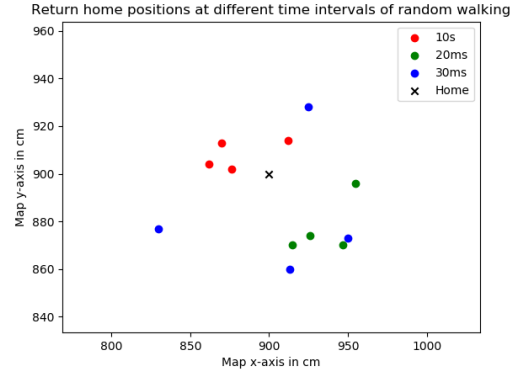


Fig. 2. Scatter plot showing robot’s ‘perceived’ origin at 3 different time periods for a random walk using kinematics for heading estimate

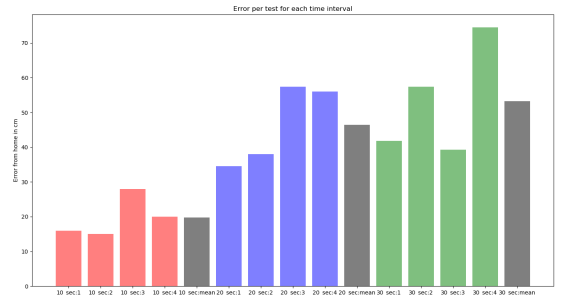


Fig. 3. Displacement error for wheel encoder odometry from Random-walk, Go Home experiment.

B. Improved Baseline Experiment: Random Walk, Go Home with Sensor Fusion

Figure 4 displays the perceived home positions for each trial for a specific random walk duration. Figure 5 illustrates the displacement error from the perceived home to the true origin for each trial as well as a mean displacement error for that random walk time period. There is a marked decrease in the mean displacement error with sensor fusion compared to Figure 3. The original baseline experiment consists of 4 trials per time period, whereas the sensor fused version consists of 3. It is believed that this marked decrease will be consistent in the 4th trial with sensor fusion. Therefore, in the light of these results gathered, it can be claimed that sensor fusion provides better localisation (less odometric error) when compared with the same experiment based only on wheel encoders.

To gain more information on the percentage of error accumulation in both translation and orientation, the performance of the subsystem is examined by conducting an advanced test called Unidirectional Square Path University of Michigan Benchmark test (UMBmark). The results from the UMBmark test are discussed next.

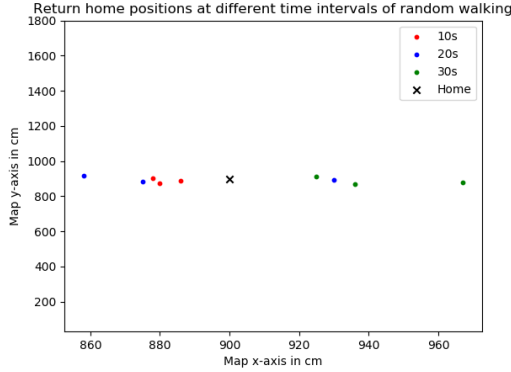


Fig. 4. Scatter plot showing robot's 'perceived' origin at 3 different time periods for a random walk using Mag-IMU sensor fusion for heading estimate

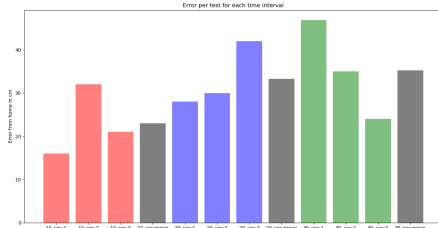


Fig. 5. Displacement error for Mag-IMU sensor fusion odometry from Random-walk, Go Home experiment

C. Unidirectional Square Path UMBmark Test

The Unidirectional UMBmark test is performed using wheel encoders for linear distance travel and heading estimates. The results from the experiment can be visualized

in Figure 7. The robot, as described earlier in the experiment design section, is programmed to traverse the four-legs of the square path three times until it returns to the starting point. Position coordinates were marked manually as the robot reached each individual point of the square. Figure 7 plots these coordinates against the true/expected coordinate points (mentioned in Figure 6) to show that the odometric error proportionally increases with the total travelled distance. The circles at each point in the plot are representative of the maximum displacement error at that point accrued over the duration of the experiment. There is a drift of the position coordinates from each corner point, which the robot has been asked to reach. This can be seen from the quadrilateral box tilting gradually away from the actual target path as the rounds are repeated. This plot also visually describes the translation and orientation errors based on either overshooting or undershooting the assigned coordinate location (displacement above or below the actual point).

| Points | X | Y | Location |
|---------|------|------|--------------|
| Point 1 | 450 | 450 | Bottom Left |
| Point 2 | 1350 | 450 | Top Left |
| Point 3 | 1350 | 1350 | Top Right |
| Point 4 | 450 | 1350 | Bottom Right |

Fig. 6. The coordinates that have been taken into consideration for the experiments across the project.

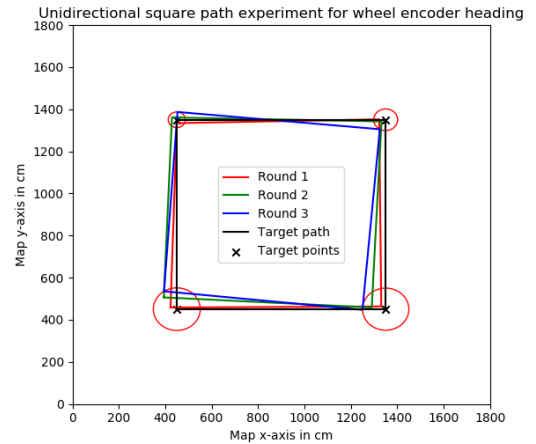


Fig. 7. Unidirectional (clockwise) UMBmark test using wheel encoders for heading estimate and linear distance travel starting from (450,450)

The results from this experiment re-affirm our understanding of the error accumulation in kinematics (wheel encoders) over time and distance travelled from the baseline experiment. Though this unidirectional UMBmark test helps in the identification of systematic error sources (unequal wheel diameters and uncertainty about the effective wheelbase) [10], this project did not focus on adding biases and thereby, reducing error caused due to these sources. Instead, this experiment is conducted to study the overall error from the

kinematic model and how effective would this model be in the task of mapping, given the unexplored environment.

It is understood that if this model is deployed on a robotic system, with the task of exploring the area with the sunken ship for 180 seconds till it has to return to its origin, the robot might end up reaching a point in the circular zone around coordinate 450,450 in the graph. However, to further crystallize this prediction, a few other independent experiments are performed to understand the approximate translational error in each point as well as the angular skew. The observed behaviour during these experiments was similar to the behaviour of the robot when performing the more complex UMBmark test.

From the results, it is understood that wheel odometry is not reliable to ensure optimum relative position estimate for spatial navigation. As a result, sensor fusion is studied to improve localisation. The magnetometer and gyroscope are used to calculate a fused heading angle that the robot uses for the path traversal task. These are done in the following combinations. Firstly, the magnetometer is investigated independently. Secondly, the magnetometer is fused with the gyroscope; and lastly, gyroscope with kinematics is used for the heading angle estimation. The results from each of these tests are analysed in the following section.

Magnetometer for heading calculation

Figure 8 illustrates the performance of the odometry subsystem with heading angle estimation using the magnetometer in the UMBmark test. There is a prominent trend of reduction in odometric error with a magnetometer as can be visualized from the graphical plot of the UMBmark path traversal task in Figure 8.

Similar to the kinematics model based experiment, three rounds of unidirectional square path traversal is conducted using a magnetometer. The readings from the magnetometer are used to calculate the orientation the robot has at different points on the square. It can be seen that the circles which represent the maximum displacement error at each point are seemingly dependent on the translation error that has been acquired over travelling a long distance (three rounds, over time). This is because the translation of the system on a linear direction is still dependent on the kinematics (wheel encoders), which as explained before, accumulates error over time.

Additionally, it is observed that there is a decrease in the error radius of the circles from Point 2 to Point 4, with the smallest circle being at Point 4. As per existing literature [14], the magnetometer is supposed give an almost perfect heading angle gradually over time, as it has a tendency for self-correction conditioned on its relative position with respect to its target. However, the magnetometer is slow and therefore, needs considerable amount of time to calculate a near perfect orientation. This progressive reduction in odometric error can only be noticed on running the experiment for long periods of time.

The magnetometer also requires calibration before use. For the purpose of this experiment, calibration was performed by

creating a ∞ shape by holding the robot above the ground to find the true magnetic north. However, the readings it averages over to calibrate itself are different from those closer to the ground, where the robot is run during the experiment. Hence, this can lead to a considerable amount of error initially. It must also be stated that the magnetometer is extremely susceptible to magnetic inference and hence, odometric improvements using magnetometers are often not recommended for indoor applications, because of the large distortions of the earth's magnetic field near power lines or steel structures [3].

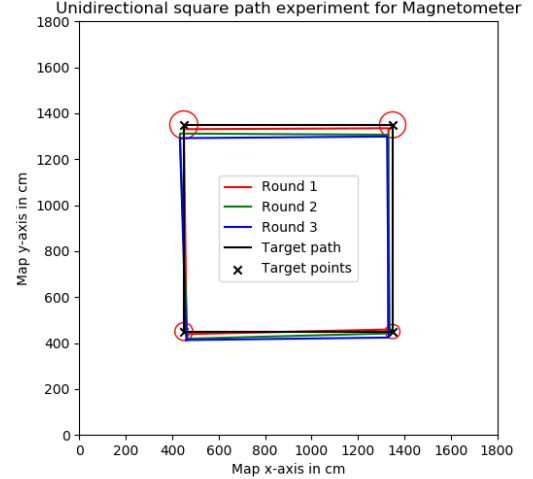


Fig. 8. UMBmark test using magnetometer to estimate heading angle in Hodgkin House

Since, all our experiments are conducted inside closed buildings, the magnetometer heading angles are not as accurate as those would be, when the experiments are performed in a quarantine place with zero or nominal magnetic inference. Nonetheless, in order to justify claimed effects of magnetic flux on the magnetometer's heading angle calculation, the same experiment was carried in two different locations, namely MVB and Hodgkin House. Figure 8 and 9 display the odometric error accumulation using the magnetometer for the heading angle calculation at the two mentioned locations. The results from MVB show an opposite pattern of error accumulation (increased error over time) against those at Hodgkin House. This unusual performance of the magnetometer based odometric subsystem is further investigated in the context of the magnetic inference at the two places. The conclusions from which are quite astonishing. MVB reports a very high magnetic field fluctuation (magnitude of raw magnetometer values in Gauss), whereas the magnitude values in Gauss at Hodgkin House do not fluctuate as much. Figure 10 shows the heat map built on the Gauss readings at the MVB and Hodgkin House.

The highly fluctuating values on the heat-map at MVB, could be attributed to the underfloor wiring and magnetic field disturbances created from the abundance of electronics used in the building, which were to some extent absent in

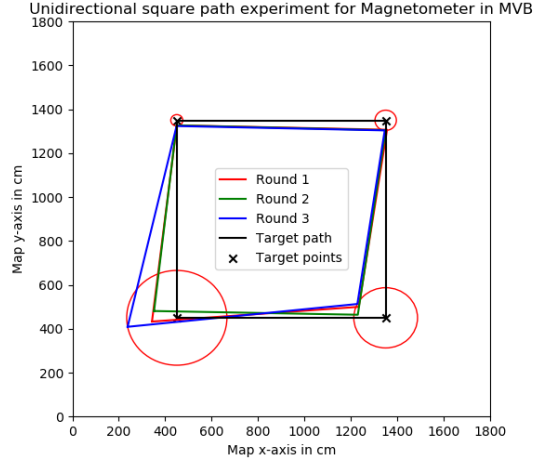


Fig. 9. UMBmark test using magnetometer to estimate heading angle in MVB

Magnetometer Values at Hodgkin House:

| | 1350, 450 | 1350, 900 | 1350, 1350 | |
|-----------|-----------|-----------|------------|--------|
| 1350, 450 | 19,100 | 18,100 | 18,400 | 18,900 |
| | 19,000 | | | 20,100 |
| 900, 450 | 18,700 | | 900, 900 | 20,500 |
| | 18,500 | | | 20,900 |
| 450, 450 | 18,300 | 20,300 | 20,300 | 20,400 |
| | | | | 20,700 |
| | 450, 450 | 450, 900 | 450, 1350 | |

Magnetometer Values at MVB:

| | 1350, 450 | 1350, 900 | 1350, 1350 | |
|-----------|-----------|-----------|------------|--------|
| 1350, 450 | 8,200 | 36,100 | 11,500 | 25,400 |
| | 20,500 | | | 22,200 |
| 900, 450 | 17,200 | | 900, 900 | 21,800 |
| | 41,000 | | | 25,200 |
| 450, 450 | 21,100 | 35,700 | 34,800 | 18,500 |
| | | | | 18,100 |
| | 450, 450 | 450, 900 | 450, 1350 | |

Fig. 10. Magnetic field values across both the locations (in Gauss)

Hodgkin House. Nevertheless, a fluctuation of 2700 Gauss is still recorded inside Hodgkin House, at different points on the path used for experimentation. This leads to re-iteration of the fact that a magnetometer would give near-perfect headings only in environments with zero or low magnetic inference. The experiment at Hodgkin House, can thus, not be categorized as a quarantine environment. Consequently, the orientation error is therefore not zero, but significantly less than that in MVB.

Magnetometer fused with gyroscope for heading calculation

Based on known issues that the magnetometer suffers from, the next logical step is to incorporate sensor fusion by fusing the gyroscope heading values with the magnetometer. It is believed that the gyroscope might counterbalance the orientation error from the magnetometer, so as to make it environment independent. Figure 11 displays results from the UMBmark test with a fused heading estimate using the magnetometer and gyroscope at Hodgkin House. Figure 12 shows odometric performance results from the UMBmark test at MVB with the same sensor fusion.

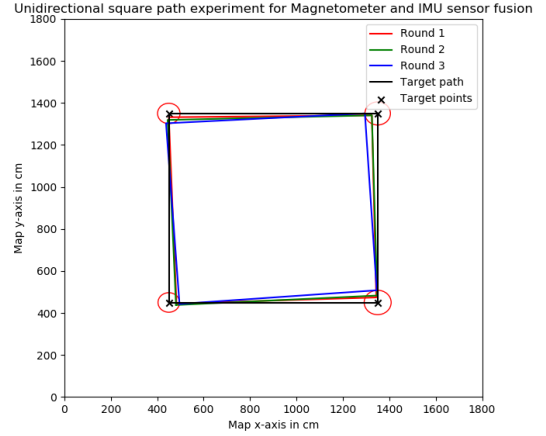


Fig. 11. UMBmark test using IMU and magnetometer fusion to estimate heading angle in Hodgkin House

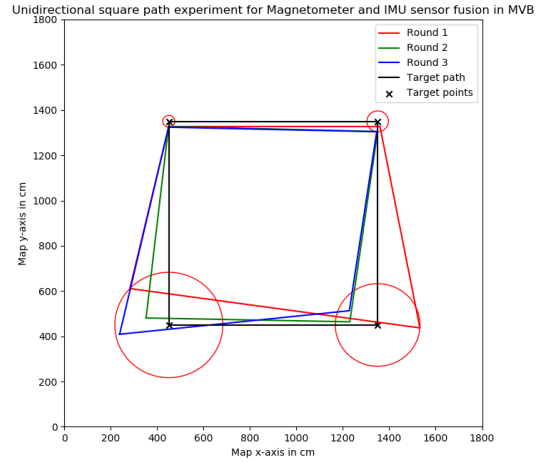


Fig. 12. UMBmark test using IMU and magnetometer fusion to estimate heading angle in MVB

The displacement error circles on Figure 11 are nearly consistent on each point, while almost displaying an optimal path traversal over time. Contrarily, Figure 12 maintains the same pattern of incremental displacement error due to high magnetic inference at MVB, as is observed in the previous experiment using only the magnetometer to calculate the heading angle of the robot. This implies that sensor fusion using the gyroscope to compensate for the magnetometer orientation error does not lead to any improvement in MVB. This is because of the persistent and predominant magnetic inference. Additionally, it should also be mentioned that for this sensor fusion experiment, the magnetometer is allocated a higher weightage than the gyroscope. This was due to authenticity and consistency of the absolute magnetometer readings [21], as opposed to the integrated odometry values from angular velocities of the gyroscope.

On comparison with the previous Figures 8 and 9, it

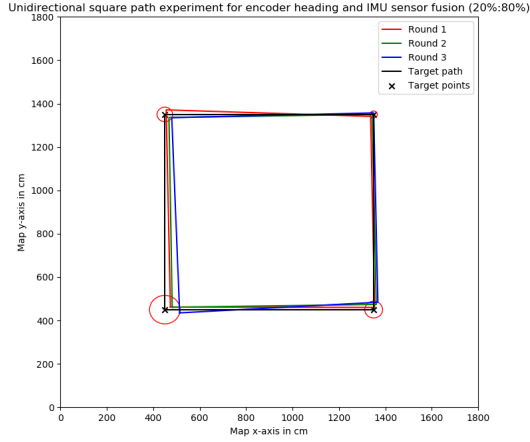


Fig. 13. UMBmark test using IMU and kinematics fusion (80:20) to estimate heading angle

can be noticed that with sensor fusion the displacement error circles are marginally larger. This can be reasoned with stating that the gyroscope employed at this stage also accumulates error on integrating the angular velocities over time during rounds of the UMBmark test. The above analysis leads to the final combination of the IMU (only gyroscope) with the wheel encoders (kinematics).

Gyroscope fused with Wheel Encoders for heading calculation

The UMBmark test is performed using heading estimates from sensor fusion of wheel encoders and IMU (gyroscope). The results are presented in Figures 13 and 14. Displacement error circle around the start/end point have the highest radius in comparison to all other points on the graph. This is assumed to be due to augmented kinematics error over time, as is observed from the previous experiments. However, it is still unclear what percentage of error was caused due to the gyroscope, which for this experiment has the maximum weight. Thus, to understand and confirm the actual effects of gyroscope and kinematics, another UMBmark test is conducted with different weights assigned to the gyroscope and kinematics than for this experiment.

Figure 14 displays UMBmark test using heading estimate from fusing IMU (gyroscope 95% weightage) with wheel encoders. The displacement error at the start/end point is lower when compared with Figure 13. The values seem to be more consistent in the Figure 14, displaying a general pattern of increase in error as the robot moves from the start and returns back while taking a clockwise path. This general trend of growing error was defied in Figure 13, which showed an unknown decrease in error at point 3 (top-right). After analysing results from this experiment, it is concluded that kinematics is causing the error propagation at the start/end position in Figure 13.

Overall, sensor fusion to improve the odometry estimation with the gyroscope (95%) and kinematics (5%) performs

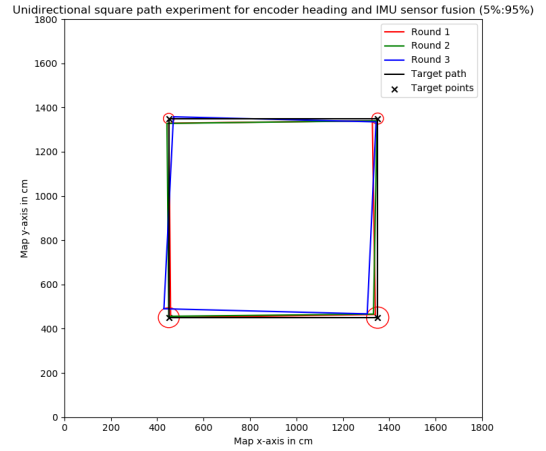


Fig. 14. UMBmark test using IMU and kinematics fusion (95:5) to estimate heading angle

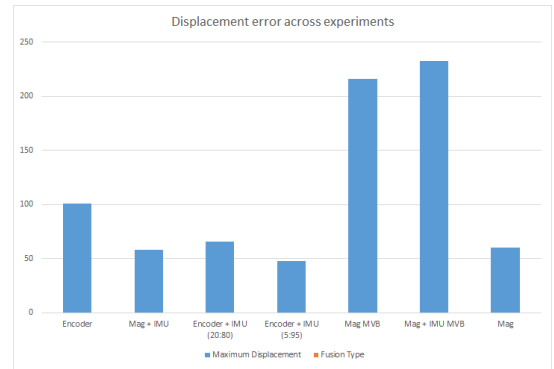


Fig. 15. Maximum displacement error across the experiments

the best with respect to all other experiments performed (as seen in Figure 15). The maximum displacement error from fusion of the magnetometer and gyroscope is found similar to that from using the magnetometer in isolation. This is because of the magnetometer's ability to correct its orientation over time, thereby mitigating the error from the gyroscope. However, the magnetometer's ideal behaviour is dependent on the environmental location and cannot be used in areas with high magnetic interference. Figure 15 illustrates the maximum displacement error from each combination of sensor fusion techniques employed for this project.

IMU (gyroscope) fusion with kinematics does work well in the context of how the experiments have been conducted for this project. Nevertheless, there seems to be an evident trend of error accumulation on returning to the start point, which can be a serious problem if the robot is assigned the task of exploring a very large area, causing it to travel too far from the start point. Presumably, the robot might not be able to return anywhere near the observed error zone around the start position until the displacement error zone calculation has been expanded through prior experiments for very long distances. Thus, it can be said that the odometric subsystem

improvements are scenario dependent and it is recommended that sensor fusion types are changed based on the exploration area.

V. EFFECT ON MAPPING

To study the impact of sensor fusion on the mapping of the region explored, maps from kinematics, kinematics and IMU fusion and IMU and magnetometer fusion are generated. These are displayed in Figures 16, 17 and 18. The travelled points on the map are denoted by ‘ \star ’ and the unexplored positions on the map are denoted by ‘ $\#$ ’. The path followed by the robot resembles a square in all three maps. The square shape is much distorted in Figure 18, which is from three rounds run of the UMBmark test using heading angle from magnetometer and IMU. The distortion occurs because of the dominant orientation error caused from the magnetometer due to magnetic interference. Additionally, since the robot traverses the same path multiple times, the stars (‘ \star ’) are generally overwritten if the robot maintains minimum error after each round on each point. This can be visualized from Figure 17, which shows the map generated from the experiment that used orientation calculation from fusion of kinematics and IMU. This map offers significant improvement against the map created using only kinematics, which is displayed in Figure 16. The shape of the square path is almost intact with minor errors in Figure 17. This implies that sensor fusion using kinematics and IMU improves the mapping accuracy of the robot more than fusion of IMU with magnetometer or the magnetometer in isolation, which supports with the results discussed in the previous section of the report.

VI. FINAL DISCUSSION

This paper presents a method for correction of the heading direction estimate to improve the odometry subsystem of the Romi robot. This paper accounts for both systematic and random error. Systematic error is successfully removed by calibration. Random error is significantly reduced by sensor fusion using a complementary filter. To test the efficiency of the sensor fusion filter, two type of tests were performed Random-walk, Go Home as well as the UMBmark test. The latter being a more structured test which helps in identifying minute inaccuracies in the robot's odometry.

In terms of measuring heading, 3 methods have been utilised. The magnetometer provides accurate readings with a variability of $\pm 10^\circ$, when in a quarantine area with minimal magnetic interference. The readings from the gyroscope, however, reduce in accuracy over time, offer extremely

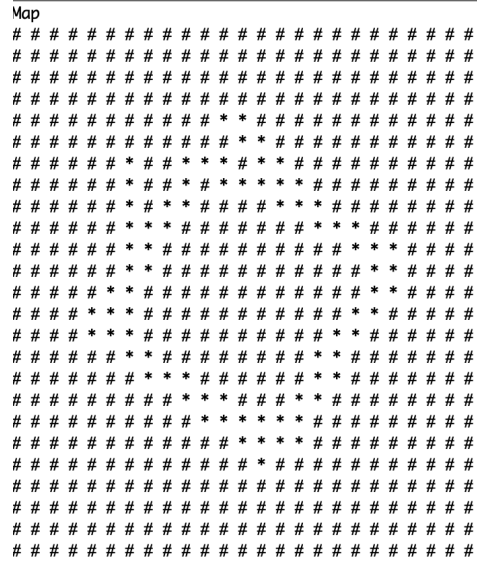


Fig. 16. Map created by the robot using heading from kinematics

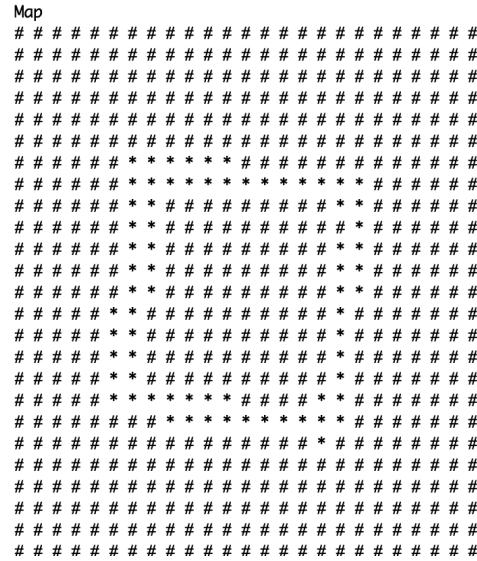


Fig. 17. Map created by the robot using heading from sensor fusion of IMU and kinematics

accurate readings for the initial brief time period. Heading determined from wheel encoders acts as a baseline, with evident accumulation of error over time. The fusion of both the gyroscope and the magnetometer theoretically provide a more accurate odometry subsystem. However, this cannot be concluded from the results, as magnetic interference appears to be a prevalent issue. From the experimental analysis show that the most significant improvement of the odometry subsystem was found with the fusion of the wheel encoders with gyroscope (5% and 95% weight respectively). This improved localisation can also be seen on the map generated by the robot (Figures 14, 17).

On the whole, from the aforementioned maps, it can be noticed that there is significant improvement on the localisation of the robot with sensor fusion as compared to

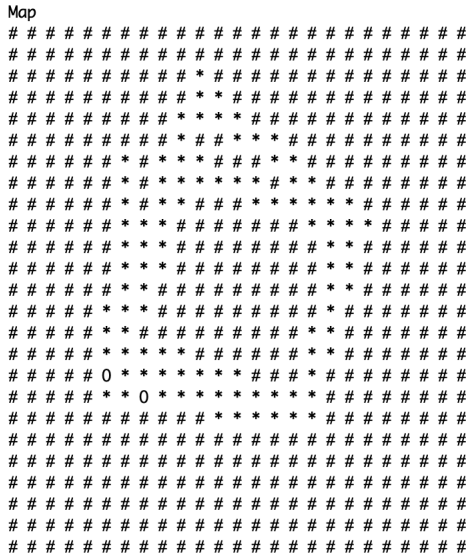


Fig. 18. Map created by the robot using heading from sensor fusion of IMU and magnetometer

only using wheel sensors based odometry. In other words, there is now less uncertainty with respect to its relative position estimate based on the starting point. Consequently, it can be claimed that if these odometric improvements of sensor fusion — magnetometer or IMU and kinematics – are used for the real exploratory task, there will be observable benefits in encoding the locations that the robot reaches during the 180 seconds of exploration. With precise and accurate localisation of the robot, other integrated sensors would estimate the location of other undersea features such as prominent rocks (obstacles), pipelines (lines) and scattered ship debris (RFID tags) with optimum accuracy and minimum uncertainty.

Significantly improved odometry would have compound-benefits in effectively describing the area with the help of other sensors as well as finding the treasure’s accurate location. It is also worth remembering that the odometric improvement models with magnetometer might not work efficiently in the regions with undersea pipelines and tons of scattered steel structures from the wrecked ship. However, this technique should work in near-accurate estimation of prominent rocks. However, the exact observations can only be deduced after actual deployment of the robots in the given scenario.

VII. FUTURE WORK

For future work it is recommended to implement further sensor fusion for identifying features on the map. Visual odometry using IR sensors [22][23] may also be used for accurately estimating the location of an obstacle while localising the robot on a map. For calculating distance travelled by the robot, it is possible to use an accelerometer (from the IMU) or a fusion of accelerometer with wheel encoders. Additionally, it is ideal to let the experiments involving the magnetometer run for a longer duration. Improvements

in sensor fusion can also be performed by implementing extended Kalman filter [17] which would provide a dynamic filter weightage unlike the complementary filter.

REFERENCES

- [1] LEVITT and T S. Qualitative navigation for mobile robots. *Int. J. Artificial Intelligence*, 44:305–360, 1990.
- [2] Matthew Grimes and Yann Le Cun. Efficient Off-Road localization using visually corrected odometry.
- [3] J Borenstein and L Feng. Gyrodometry: a new method for combining data from gyros and odometry in mobile robots. In *Proceedings of IEEE International Conference on Robotics and Automation*, volume 1, pages 423–428 vol.1, April 1996.
- [4] Kok Seng Chong and L Kleeman. Accurate odometry and error modelling for a mobile robot. In *Proceedings of International Conference on Robotics and Automation*, volume 4, pages 2783–2788 vol.4, April 1997.
- [5] J Borenstein and Liqiang Feng. Correction of systematic odometry errors in mobile robots. In *Proceedings 1995 IEEE/RSJ International Conference on Intelligent Robots and Systems. Human Robot Interaction and Cooperative Robots*, volume 3, pages 569–574 vol.3, August 1995.
- [6] L C Bento, U Nunes, F Moita, and A Surrecio. Sensor fusion for precise autonomous vehicle navigation in outdoor semi-structured environments. In *Intelligent Transportation Systems, 2005. Proceedings. 2005 IEEE*, pages 245–250, October 2005.
- [7] Steven Daniluk. Ghost IV — sensor fusion: Encoders + IMU – hacker noon. <https://hackernoon.com/ghost-iv-sensor-fusion-encoders-imu-c099dd40a7b>, March 2017. Accessed: 2019-5-14.
- [8] Radosław Cechowicz. Bias drift estimation for MEMS gyroscope used in inertial navigation. *Acta Mechanica et Automatica*, 11(2):104–110, June 2017.
- [9] Manon Kok, Jeroen D Hol, and Thomas B Schön. Using inertial sensors for position and orientation estimation. April 2017.
- [10] J Borenstein and L Feng. A method for measuring, comparing, and correct- ing dead-reckoning errors in mobile robots.
- [11] Changbae Jung and Woojin Chung. Design of test tracks for odometry calibration of wheeled mobile robots. *Int. J. Adv. Rob. Syst.*, 8(4):56, September 2011.
- [12] Hatem Alismail and Brett Browning. Exploring visual odometry for mobile robots, 2009.
- [13] Pololu - LIS3MDL 3-axis magnetometer carrier with voltage regulator. <https://www.pololu.com/product/2737>. Accessed: 2019-5-14.
- [14] Marcio Barata, Urbano Nunes, L Conde Bento, and Abel Mendes. Data fusion of wheel encoders and magnetic sensors for autonomous vehicles navigation. In *Intelligent Transportation Systems, 2005. Proceedings. 2005 IEEE*, September 2005.
- [15] Pololu - accelerometers, gyros, & compasses. <https://www.pololu.com/category/80/accelerometers-gyros-compasses>. Accessed: 2019-5-14.
- [16] Raymond H Byrne, P R Kiarer, and J Bryan Pletta. Techniques for autonomous navigation. *undefined*, 1992.
- [17] Tariqul Islam, Md Saiful Islam, Shajid-Ul-Mahmud, and Hossam-E-Haider. Comparison of complementary and kalman filter based data fusion for attitude heading reference system. *AIP Conf. Proc.*, 1919(1):020002, December 2017.
- [18] Guest. Quantitative performance metrics for mobile robots navigation - PDF free download. <https://zdoc.site/quantitative-performance-metrics-for-mobile-robots-navigatio.html>, May 2019. Accessed: 2019-5-14.
- [19] Timothy A Zimmerman. Metrics and key performance indicators for robotic cybersecurity performance analysis. Technical report, National Institute of Standards and Technology, Gaithersburg, MD, April 2017.
- [20] A Lampe and R Chatila. Performance measure for the evaluation of mobile robot autonomy. In *Robotics and Automation, 2006. ICRA 2006. Proceedings 2006 IEEE International Conference on*, pages 4057–4062, June 2006.
- [21] Estefania Munoz Diaz, Fabian de Ponte Müller, and Juan Jesús García Domínguez. Use of the magnetic field for improving gyroscopes’ biases estimation. *Sensors*, 17(4), April 2017.
- [22] N Nourani-Vatani, J Roberts, and M V Srinivasan. Practical visual odometry for car-like vehicles. In *Robotics and Automation, 2009. ICRA '09. IEEE International Conference on*, pages 3551–3557, June 2009.

- [23] Mohammad O A Aqel, Mohammad H Marhaban, M Iqbal Saripan, and Napsiah Bt Ismail. Review of visual odometry: types, approaches, challenges, and applications. *Springerplus*, 5(1):1897, October 2016.